

Title	A Method of Topographical Correction upon the Intensity of Gravity and its Application to the Intensity of Vertical Gradient of Gravity
Author(s)	Abe, Etsuo
Citation	Memoirs of the Faculty of Science, Kyoto University. Series of geology and mineralogy (1971), 38(1): 135-153
Issue Date	1971-08-15
URL	<a href="http://hdl.handle.net/2433/186574">http://hdl.handle.net/2433/186574</a>
Right	
Type	Departmental Bulletin Paper
Textversion	publisher

## A Method of Topographical Correction upon the Intensity of Gravity and its Application to the Intensity of Vertical Gradient of Gravity

By

Etsuo ABE

(Received April 13, 1971)

### Abstract

In this paper a new method of computing topographic effect upon the intensity of gravity determined at the earth's surface is described. The computation of topographic effect is done by tables of which the tabular values of the effect are obtained in microgal in order to meet the sensitivity of the modern gravimeter, 0.01 milligal(mgal) or 10 microgal( $\mu$ gal).

In this method the area around a gravity station is divided into 300 sectorial compartments by 26 concentric circles with the center at the station and 12 equally spaced radial lines passing through it. Radius of the circle increases with the common ratio  $\beta$  which is 1.5849, the smallest and the largest radii being respectively 1 m and 100 km.

A transparent graticule, on which the above concentric circles and radial lines are drawn, is placed on a topographic map with a center at the gravity station represented on the map. The mean height of land surface within each compartment is estimated. The vertical attraction of each sectorial compartment block with its height equal to the above obtained mean height is computed in microgal by the tables and by assuming an appropriate value to the density of the block.

The accuracy of the value of the attraction thus obtained by the tables is examined by employing a model topography of which the vertical attraction at the station can be exactly calculated other than by the tables. The result is that the tabular value differs from the exact value by a little less than 0.1 mgal. The computation tables for gravity is applicable to the topographical correction upon the intensity of vertical gradient of gravity which is obtained by  $(g_1 - g_2)/\delta z$ , where  $g_1$  is the gravity value at a ground station and  $g_2$  at a station at a height  $\delta z$  vertically above the former.

Convenient tables for obtaining the effect of near topography which may be treated as two-dimensional are obtained.

At four selected stations in the mountainous area of the central Honshû of Japan, the topographic corrections have been done by the tables mentioned above upon the intensities of gravity and its vertical gradient, and the values of the Modified Bouguer anomaly at sea-level at these stations have been obtained to prove that the Simple Bouguer anomalies at stations in a lofty mountainous area are dangerous as data to find the state of isostatic equilibrium or, generally speaking, the mass distribution below such an area.

### Introduction

Since the appearance of gravimeters with an accuracy of 0.01 mgal, the

gravimetric research of subsurface geological structure and particularly the gravimetric prospecting of underground natural resources have been speedily developed. In order to infer a subsurface geological structure from the values of gravity measured on the ground surface, they must be submitted to the well-known three different corrections, namely 1) topographical correction, 2) Bouguer correction and 3) free-air correction. Among them the topographical correction is indispensable for making the best use of modern gravimeter accuracy of 0.01 mgal. In this paper is described the author's new method of topographical correction. For finding the errors involved in the topographical value at a gravity station computed by the tables which the author has constructed in this paper, they were applied to a model topography which is an assemblage to form a pyramid of simple sectorial blocks of which the vertical attraction at the same station can be exactly calculated. The error thus found was 0.07~0.11 mgal. For obtaining this error, the effect of the uncertainty in the assumption of the density of blocks is not considered in this paper.

### §1. Method of topographic correction

Different methods of topographical correction for the intensity of gravity have been published by several authors such as Hayford (1912), Bowie (1917), Jung (1927), Bullard (1936), Hammer (1939), Fuchida (1948) and Matsuda (1952). The method described in this paper is based on the following principle, which is similar to the Hammer's method which may be most convenient to usage according to the author's experiences. The whole area (in a given topographic map) within a circle of radius 100 km from the gravity station, is divided by a number of concentric circles with the common center at the gravity station and equally separated radial lines drawn from the station to form a great number of sectorial compartments. The mean height of the topography in each compartment is estimated. The vertical attraction at the gravity station of the compartment block, of which the height is equal to the mean height, can be computed exactly. The summation of the vertical attractions of all the compartment blocks is the required topographical correction at the gravity station. The error involved in the thus obtained correction arises from the adoption of the mean height instead of the actual topography and also from the assumption of the density of the compartment block.

For a distant topography beyond 100 km from the gravity station, a different method of correction should be adopted taking the earth's curvature into consideration. This is out of the scope of this paper.

If  $r_m$  and  $r_{m+1}$  are respectively the inner and outer radius of the compartment block, which is standing above the horizontal plane passing through a gravity

station  $P$  at the height  $H$  above the sea-level,  $2\pi/N$  the angular width of each compartment,  $h$  the height of the compartment block above the sea-level, and  $\sigma$  the density of the block, the vertically downward attraction  $\Gamma_m$  at the gravity station of the block is, the axis of  $Z$  being directed in the vertically downward direction (Fig. 1),

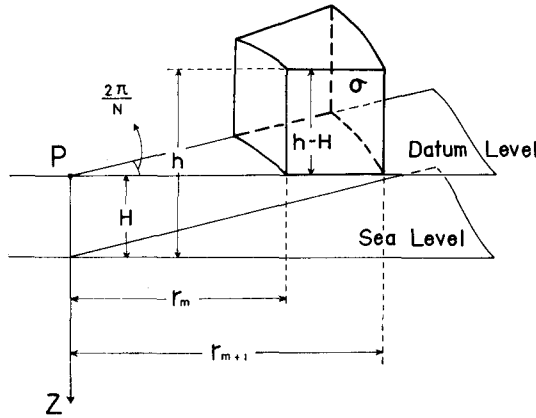


Fig. 1.

$$\Gamma_m = -\frac{2\pi\tau}{N} \cdot \sigma \cdot \{r_{m+1} - r_m + \sqrt{r_m^2 + (h-H)^2} - \sqrt{r_{m+1}^2 + (h-H)^2}\}, \quad \dots(1)$$

where  $\tau$  is the attraction constant, for which let us use the  $6.67_3 \times 10^{-8}$  c.g.s.. In the following let us establish the values for  $N$  and  $r_m$  and  $r_{m+1}$  for the sake of making the table of the values of  $\Gamma_m$ . At the outset let us employ

$$\frac{1}{r_m} - \frac{1}{r_{m+1}} = \alpha \frac{1}{r_m}, \quad \dots\dots\dots(2)$$

where  $\alpha$  is a constant. From the Eq. (2) follows

$$\frac{r_{m+1}}{r_m} = \frac{1}{1-\alpha} = \beta, \quad \dots\dots\dots(3)$$

where  $\beta$  is another constant depending on  $\alpha$ . Then, for the first  $n$  ones of the whole concentric circles  $m$  takes the values of 1, 2,  $\dots$ ,  $n$ , and from the Eq. (3) we get

$$\left. \begin{aligned} r_2 &= \beta r_1 \\ r_3 &= \beta^2 r_1 \\ &\vdots \\ r_n &= \beta^{n-1} r_1. \end{aligned} \right\} \dots\dots\dots(4)$$

Further assuming

$$r_n = 10r_1, \dots\dots\dots(5)$$

we obtain

$$(n-1) \log_{10} \beta = 1 \quad \text{or} \quad \beta = 10^{1/(n-1)} \dots\dots\dots(6)$$

If for the positive integer  $n$ , which is the number of the concentric circles from  $r_1$  to  $r_n=10r_1$ , a suitable value is selected, the value of  $\beta$  can be determined from the Eq. (6), and all the values of  $r_1, r_2, \dots, r_n$  can be done from the Eq. (4). Now next, let us determine the value of  $N$ , the number of the radial lines equally separated. If we require that the shape of each compartment should be approximately a square,  $N$  is an integer nearest to the value of  $N'$  given by the Eq. (7)

$$N' = \frac{r_{m+1} + r_m}{r_{m+1} - r_m} = \pi \cdot \frac{\beta + 1}{\beta - 1} \dots\dots\dots(7)$$

Next, let us proceed to find a suitable value for  $n$ . If we adopt a smaller value for  $n$ , the value of  $\beta$  increases to produce a smaller value for  $N'$  and, therefore, for  $N$ , as  $dN'/d\beta$  is a negative quantity. The smaller is the value of  $n$  and, therefore, of  $N$ , the smaller is the number of the total compartment. This means the increasing of the speed of carrying out the topographical correction. However, this means the decreasing of its accuracy, because the error of the adoption of the mean height for the compartment against the adoption of the actual topography increases. Therefore, the efficiency and the accuracy of the topographical correction are contrary to each other. Selection of a suitable value for  $n$  is subject to this condition.

**§2. Tabulation of the values of  $\Gamma_m$**

From the condition shown in the end of the foregoing article, the author has employed a value of 6 for  $n$ . By means of this value of  $n$ , the Eqs. (6) and (7) give rise to  $\beta=1.5849$  and  $N=12$  respectively. From the author's experience, these values of  $n$  and  $N$  are appropriate to the usual topography. Now letting the radii of the 6 concentric circles be  $r_1, r_2, \dots, r_6 (=10r_1)$ , and starting from  $r_1=1\text{m}$ , we get

$$\left. \begin{aligned} r_1 &= 1.0000 \text{ m} \\ r_2 &= 1.5849 \text{ m} \\ r_3 &= 2.5119 \text{ m} \\ r_4 &= 3.9811 \text{ m} \\ r_5 &= 6.3096 \text{ m} \\ r_6 &= 10.0000 \text{ m} . \end{aligned} \right\} \dots\dots\dots(8)$$

These six values of  $r_s$  given by the Eq. (8) belong to the first six concentric circles which are nearest to the gravity station.

Let the zone bounded by the two concentric circles of radii  $r_1=1.0000$  m and  $r_6=10.0000$  m be called A zone, beyond which there are 4 zones called B, C, D and E zones. The smallest radius of each zone is equal to the greatest radius of the preceding zone. This scheme is as follows:

$$\left. \begin{aligned} r_1 &= 1 \text{ m} \sim r_6 = 10 \text{ m} \text{ --- A zone} \\ r_1 &= 10 \text{ m} \sim r_6 = 100 \text{ m} \text{ --- B zone} \\ r_1 &= 100 \text{ m} \sim r_6 = 1 \text{ km} \text{ --- C zone} \\ r_1 &= 1 \text{ km} \sim r_6 = 10 \text{ km} \text{ --- D zone} \\ r_1 &= 10 \text{ km} \sim r_6 = 100 \text{ km} \text{ --- E zone,} \end{aligned} \right\} \dots\dots\dots (9)$$

where the values of the intermediate radii  $r_2, r_3, r_4$  and  $r_5$  of any zone are ten times those of the preceding zone. The Eq. (1) can be rewritten as

$$\Gamma_m = -\frac{2\pi\gamma}{N} \cdot \sigma \cdot r_m \cdot \left\{ \beta - 1 + \sqrt{1 + \left(\frac{h-H}{r_m}\right)^2} - \sqrt{\beta^2 + \left(\frac{h-H}{r_m}\right)^2} \right\}, \dots (10)$$

For simplicity's sake let us put

$$f_m = -\frac{2\pi\gamma}{N} \cdot r_m \cdot \left\{ \beta - 1 + \sqrt{1 + \left(\frac{h-H}{r_m}\right)^2} - \sqrt{\beta^2 + \left(\frac{h-H}{r_m}\right)^2} \right\}, \dots\dots (11)$$

when  $(h-H) > 0$  (Fig. 2(a)), the density  $\sigma$  is positive, and in this case (11) takes the form

$$\Gamma_m = f_m \cdot \sigma \dots\dots\dots (12)$$

The Eq. (11) also holds for the case in which  $(h-H) < 0$  and  $\sigma < 0$ , i.e., for the case of empty block (Fig. 2(b)), because in this case, for calculating  $\Gamma_m$ , the integration with respect to  $Z$  is done from  $(h-H)$  to 0, whereas in the former case the same integration is from 0 to  $(h-H)$ .

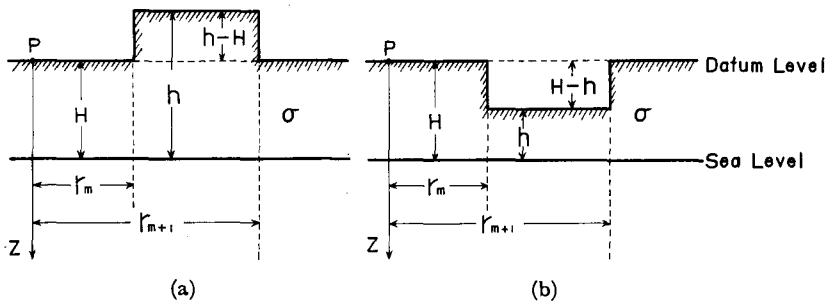


Fig. 2.

Therefore, for both the cases the same Eq. (12) holds. Since in the expression of  $f_m$  the quantity  $h-H$  appears as  $(h-H)^2$ , for both the real and empty blocks only the absolute value  $|h-H|$  is concerned. As shown by the Eq. (12),  $\Gamma_m$  is proportional to  $\sigma$ , the table for  $\Gamma_m$  may be constructed for  $\sigma=1.00 \text{ gm} \cdot \text{cm}^{-3}$ , that is the table of  $f_m$  of which the unit in c.g.s. is  $\text{gal}/\text{gm} \cdot \text{cm}^{-3}$ . As shown by the Eq. (11),  $f_m$  depends on the ratio of  $h-H/r_m$ , so that the table of  $f_m$  may be constructed for successive value of this ratio appropriately employed. Each zone of A, B, C, D and E is divided into 5 subzones bounded by the 6 concentric circles of the radii  $r_1, r_2, r_3, r_4, r_5$  and  $r_6 (=10r_1)$ , and these 5 subzones are called the subzone I, II, III, IV and V. The values of  $f_I, f_{II}, f_{III}, f_{IV}$  and  $f_V$ , of which the suffixes indicate the subzones, are then to be tabulated. At the outset, by the Eq. (11) in which  $N=12$  and  $\beta=1.5849$ , the values of  $f_I$  of the most distant zone E were calculated in  $\mu\text{gal}$  ( $=10^{-3}\text{mgal}$ ) for every 0.001 of the ratio  $|h-H|/r_1$  for the range from 0.001 to 0.500 and with  $r_1=10,000 \text{ m}$ . Multiplying these values of  $|h-H|/r_1$  by 10,000 m, we obtained values of  $|h-H|$  in meter. Then was constructed the table of  $f_I$  of the same zone E for every 10 m of  $|h-H|$  ranging from 10 m to 5,000 m. Next, the values of  $f_{II}$  of the same zone E were found by making use of those of  $f_I$  thus obtained by a method as described in the following. For a moment let us denote the values of  $|h-H|$  of a compartment of the subzone I and that of II by  $|h-H|_I$  and  $|h-H|_{II}$  respectively. Then, if  $|h-H|_{II}=\beta|h-H|_I$ , we have  $|h-H|_{II}/r_2=|h-H|_I/r_1$ , owing to  $r_2=\beta r_1$ , and, therefore, the value of  $f_{II}$  for such a value of  $|h-H|_{II}$  is equal to the value of  $\beta f_I$  for the above value of  $|h-H|_I$  ( $=|h-H|_{II}/\beta$ ). Consequently, it was able to draw a curve to represent a variation of  $f_{II}$  vs.  $|h-H|_{II}$ . The curve thus drawn was almost linear except for the vicinity of the origin to ensure us an accurate interpolation of the curve. From this interpolation, which had been most accurately carried out, we obtained the values of  $f_{II}$  for every 20 m of  $|h-H|$  from 20 m to 7,980 m to construct the table of  $f_{II}$ . From the table of  $f_I$ , was in the similar way constructed the table of  $f_{III}$  for every 25 m of  $|h-H|$  from 25 m to 12,575 m by employing the multiplier  $\beta^2$  instead of  $\beta$  which had been employed in the construction of the table of  $f_{II}$ , the table of  $f_{IV}$  for every 50 m of  $|h-H|$  from 50 m to 19,900 m by employing the multiplier  $\beta^3$ , and finally the table of  $f_V$  for every 50 m of  $|h-H|$  from 50 m to 31,550 m by employing the multiplier  $\beta^4$ . Thus the five tables of  $f_I, f_{II}, f_{III}, f_{IV}$  and  $f_V$  all belonging to the zone E were completed.

The similar five tables belonging to the remaining zones D, C, B and A (the nearest zone) can be easily obtained, owing to the functional working of the parameter  $r_m$  in the Eq. (11), by simple, successive shifts in the leftward direction of the decimal points of the tabular figures of  $|h-H|$  and  $f_m$  ( $m=I, II, III, IV$  and  $V$ ) of the successively preceding zones E, D, C and B respectively.

The total results for all the zones A, B, C, D and E are given in Tables I-1, 2, 3, 4 and 5 filed in the end of this paper. The usage of the tables will be explained with the following examples. 1) Let the value of  $|h-H|$  of a compartment bounded by two radial lines separated by an angle of  $30^\circ$  in the subzone I of the zone E be 1,550 m. Then, the value of  $f_I$  for this value of  $|h-H|$  is read as 153.0  $\mu\text{gal}$  (cf. Table I-1). 2) If  $|h-H|=1,550$  m for the similar compartment in the subzone II of the same zone E, the value of  $f_{II}$  is 97.3  $\mu\text{gal}$ , the mean of the two tabular values of 96.8 and 98.5  $\mu\text{gal}$  (cf. Table I-2(a)). 3) If  $|h-H|=682$  m for the subzone III of the zone D, the value of  $f_{III}$  is equal to  $114.46 + (115.28 - 114.46) \times 2.0/2.5 = 114.46 + 0.66 = 115.12 \mu\text{gal}$  (cf. Table I-3(b) in which we have to employ the leftward shift of the decimal points by one figure of the tabular values of  $|h-H|$  and  $f_{III}$ ).

**§3. Utilization of the topographic correction tables for the intensity of vertical gradient of gravity**

It is necessary to make a precise topographical correction upon the observed values of the vertical gradient of gravity. When the gravity difference between two points lying on a vertical line with the height difference  $\delta z$  assumed to be small is  $\delta g$ , the vertical gradient of gravity at the middle of the two points, or approximately at the lower point usually taken at the ground surface, may be given by the ratio  $\delta g/\delta z$ . If the topographical effect upon the gravity value  $g_1$  at the ground surface is  $\Gamma_{(1)}$  and that upon the gravity value  $g_2$  at the higher point  $\Gamma_{(2)}$ , the value of the vertical gradient of gravity corrected for the topography is

$$\frac{(g_1 - \Gamma_{(1)}) - (g_2 - \Gamma_{(2)}^*)}{\delta z} = \frac{g_1 - g_2}{\delta z} + \frac{\Gamma_{(2)}^* - \Gamma_{(1)}}{\delta z} \dots\dots\dots (13)$$

The first term at the right side of the Eq. (13) is the observed value of the vertical gradient and the second term the topographical correction. The values of  $g_1$  and  $g_2$  can be observed with an accuracy of a few units of 0.01 mgal by using a gravimeter, so that the same accuracy is required to  $\Gamma_{(1)}$  and  $\Gamma_{(2)}$ . According to the tables of the topographical effect given in the present paper, the correctional value can be obtained at least down to the figure of 0.1  $\mu\text{gal}$  (0.0001 mgal). For the range of the topographical correction upon the vertical gradient of gravity determined by the Eq. (13), the distance of 10 km from the gravity-gradient station is usually sufficient, according to the author's experience. Then, the total number of the compartments concerned with the vertical gradient of gravity is 240. Therefore, the computation errors in  $\Gamma_{(1)}$  and  $\Gamma_{(2)}$  arising from the tabular error of  $\pm 0.0001$  mgal for each compartment is

---

\*  $\Gamma_{(2)}' = \Gamma_{(2)} - 2\pi\gamma \cdot \delta z \cdot \sigma$  ( $= 0.04193 \cdot \delta z \cdot \sigma$  mgal) (cf. §6 of this paper)



$$\pm 0.0001\sqrt{240}\sigma = \pm 0.00155\sigma \text{ mgal}, \quad \dots\dots\dots(14)$$

where  $\sigma$  is the density assumed constant for all the compartments. Hence, the error expected in  $\Gamma_{(2)} - \Gamma_{(1)}/\delta z$  is

$$\frac{\pm 0.00155\sqrt{2}}{\delta z}\sigma = \frac{\pm 0.0022}{\delta z}\sigma \text{ mgal/m}. \quad \dots\dots\dots(15)$$

The measurements of vertical gradient of gravity in Japan have been continued since Sept. of 1955. At the beginning, the value of  $\delta z$  was about 10 m when making use of fire-towers and later has been about 5 m since we began to exclusively use a jeep equipped with an extensible ladder of which the upper plate when fully extended is at a height of about 5 m above the ground surface. Therefore, the errors computed by the Eq. (15) are  $\pm 0.0002\sigma$  mgal/m and  $\pm 0.0004\sigma$  mgal/m for  $\delta z=10$  m and 5 m respectively. If we assume  $2.67 \text{ gm}\cdot\text{cm}^{-3}$  for  $\sigma$ , those values become  $\pm 0.00053$  and  $\pm 0.00106$  mgal/m. The observation error of the vertical gradient  $(g_1 - g_2)/\delta z$  observed by the gravimeter and the jeep above mentioned has been found to be in the range from  $\pm 0.001$  mgal/m (=10 Eötvöses) to  $\pm 0.002$  mgal/m (=20 Eötvöses). Therefore, the topographical correction tables obtained in this paper may be safely utilized for the topographical correction upon the intensity of vertical gradient of gravity observed with the accuracy mentioned above.

#### §4. Actual procedure of the topographic correction

Concentric circles are drawn on a transparent sheet with the radii  $r_m$  reduced to the scale of a topographical map adopted. These circles are divided into 12 equal parts by the radial lines drawn from the center to form sectorial compartments. Next, putting this center on a gravity station plotted on the topographical map, the mean heights  $h$  above the sea-level of the topography within the compartments are estimated. If the height above the sea-level of a gravity station is  $H$ , we can obtain the values of  $|h-H|$  of the compartments belonging to a selected subzone of a selected zone, from which the corresponding values of  $f_m$  can be obtained from the corresponding tables of  $f_m$  ( $m=I, II, III, IV$  and  $V$ ). Multiplying the thus obtained values of  $f_m$  with the density  $\sigma$  of the corresponding block suitably estimated by the help of geological maps, the value of the topographical effect  $\Gamma_m = f_m \cdot \sigma$  can be found. Then, the summation of all the thus obtained values  $\Gamma_m$  up to the greatest value of  $r_m$ , which is usually less than 100 km, is the topographic effect at the gravity station. Subtracting of the summation  $\Sigma \Gamma_m$  from the gravity value observed at the station means to accomplish the topographical correction.

§5. Errors of topographic correction

The errors involved in the topographical effects  $f_m \cdot \sigma (= \Gamma_m)$  obtained from Tables I-1, 2, 3, 4, 5 arise from the situation that the actual topography within each compartment is replaced by the compartment block of the mean height  $|h-H|$ . Errors also arise from the uncertainty of the density  $\sigma$  assumed to the block. However, this kind of errors is not discussed in the present paper. At first will be examined the error produced when the actual topography of a compartment has a constant slope along the radial line (Fig. 3(a) and Fig. 3(b)). If the

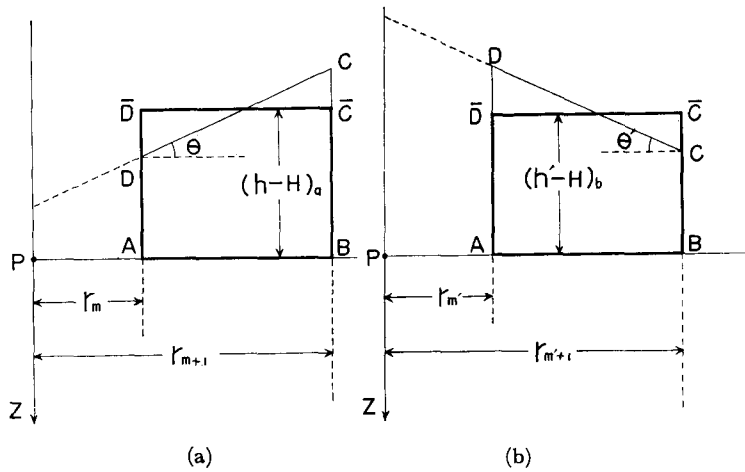


Fig. 3.

vertical attractions, directed upward and therefore negative, at a gravity station  $P$  of two compartment blocks of actual topography, whose radial cross-sections  $A B C D$  as shown in Figs. 3(a) and 3(b), are denoted by  $f_z(A B C D)_a$  and  $f_z(A B C D)_b$  respectively, and those at  $P$  of the two such equivalent compartment blocks of cross-sections  $A B \bar{C} \bar{D}$ , where  $\bar{C} \bar{D}$  is a horizontal line, that volume  $A B C D = \text{volume } A B \bar{C} \bar{D}$ , be denoted by  $f_z(A B \bar{C} \bar{D})_a$  and  $f_z(A B \bar{C} \bar{D})_b$  respectively, a simple physical consideration will easily prove

$$\left. \begin{aligned} 0 > f_z(A B C D)_a > f_z(A B \bar{C} \bar{D})_a & \quad (\text{Fig. 3(a)}) \\ f_z(A B C D)_b < f_z(A B \bar{C} \bar{D})_b < 0 & \quad (\text{Fig. 3(b)}) \end{aligned} \right\} \dots\dots\dots(16)$$

The actual topography around a gravity station is usually so irregular that, as to the radial slopes of the ground surface, the ascending slopes and descending ones are nearly, equally frequent, so that the errors arising from the replacing of the compartment blocks of actual topography with their equivalent blocks with the

mean height  $h-H$  nearly cancel each other, as can be judged by Eq. (16). Further, we have to examine the case in which the ground surface of a compartment block slopes in the direction perpendicular to the radial line. In Fig. 4, A B C D is the vertical cross-section of the block of the actual topography with a slope  $\theta$  at a distance from  $P$  equal to  $(r_m+r_{m+1})/2$ , ( $P$ ) is the projection of  $P$  on the inner

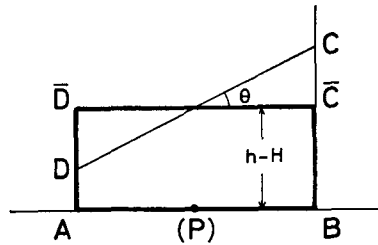


Fig. 4.

vertical wall of the block and A B C-bar D-bar is the cross-section of the equivalent block with its volume equal to that of the block A B C D. Then, simple calculation will prove that the sign of the error of the vertical attraction  $f_z(A B C\bar{D})$  against the actual one  $f_z(A B C D)$  depends on the values of  $r_m$ ,  $h-H$  and  $\theta$ , so that in the whole area of the topographical correction the occurrence of the positive and negative errors may be nearly, equally frequent and they may nearly cancel each other, just as in the case of the radial slopes. It can, therefore, be said that the replacing of the ground surface of a compartment block with the horizontal upper surface of its equivalent, equivoluminal block may not produce a large error. However, it would be necessary to examine the value of this kind of error by employing a model topography, and this will be done later on.

Before doing this examination, let us examine the influence of the error involved in the estimation of  $|h-H|$  in the case of usual topography in which  $r_m$  is generally greater than  $|h-H|$ . If the error in  $f_m$  produced by the error  $d(h-H)$  in the relative height  $h-H$  is denoted by  $df_m$ , we get by differentiating the Eq. (11) with respect to  $h-H$

$$df_m = \pm 1.2908 \cdot 10^{-6} \cdot \frac{|h-H|}{r_m} |d(h-H)| \text{ gal/gm} \cdot \text{cm}^{-3}, \dots\dots\dots (17)$$

where  $1.2908 \cdot 10^{-6}$  is the value of  $(2\pi r/N) \cdot (\beta-1)/\beta$  with the values of  $r_m$  and  $h-H$  expressed in meter. If we put  $df_m = 10^{-x}$  for one compartment, the summation of the effects of these errors for all the 276 compartments is  $10^{-x} \cdot 276^{1/2} = 10^{-x} \cdot 16.65$ . Putting this value equal to  $10^{-5}$  gal, the sensitivity of the gravity measurement by a gravimeter, we obtain  $x=6.22$  and let us adopt  $x=6$ , which produces from the Eq. (17)

$$|h-H| \cdot |d(h-H)| = 0.77471 \cdot r_m \cdot m^2, \dots\dots\dots (18)$$

which is a rectangular hyperbola with a parameter  $r_m$ , as shown by the diagrams in Fig. 5. The diagrams indicate as follows: For a given subzone of a given zone, the permissible error  $d(h-H)$  in the estimated value of  $|h-H|$  increases with decreasing value of it, and for a given value of  $|h-H|$  within a given zone

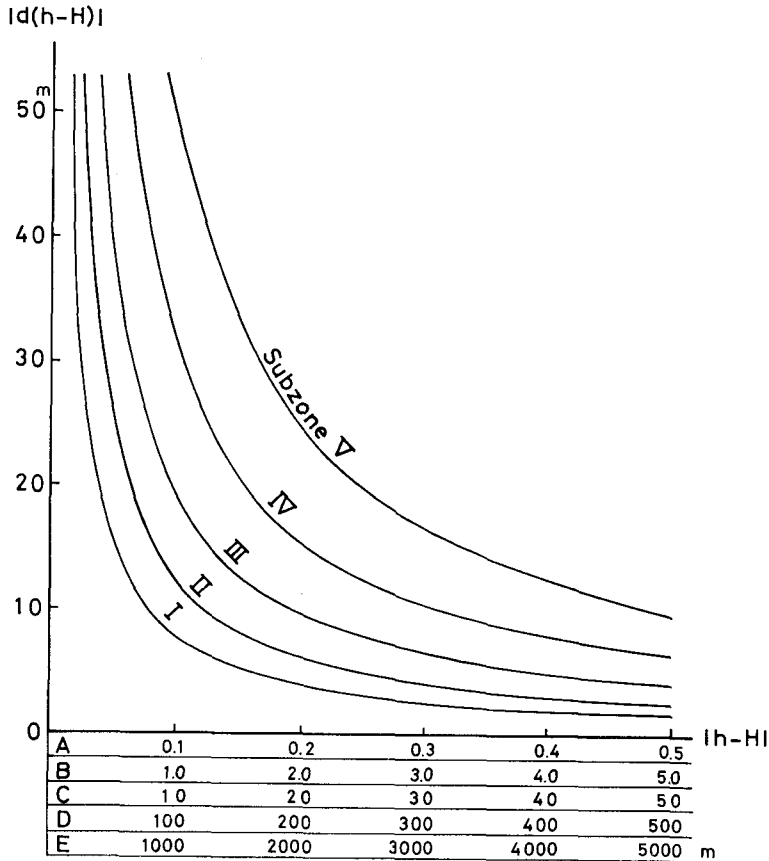


Fig. 5.

the error also increases as the distance of the subzone from the gravity station becomes greater. The ratio  $|d(h-H)|/|h-H|$  with a given value of  $|d(h-H)|$  in a given subzone increases with a common ratio of 10 as the zone approaches the gravity station. These diagrams will help a map reader in judging with what degree of accuracy the mean height  $h$  of the topography of a given compartment should be found.

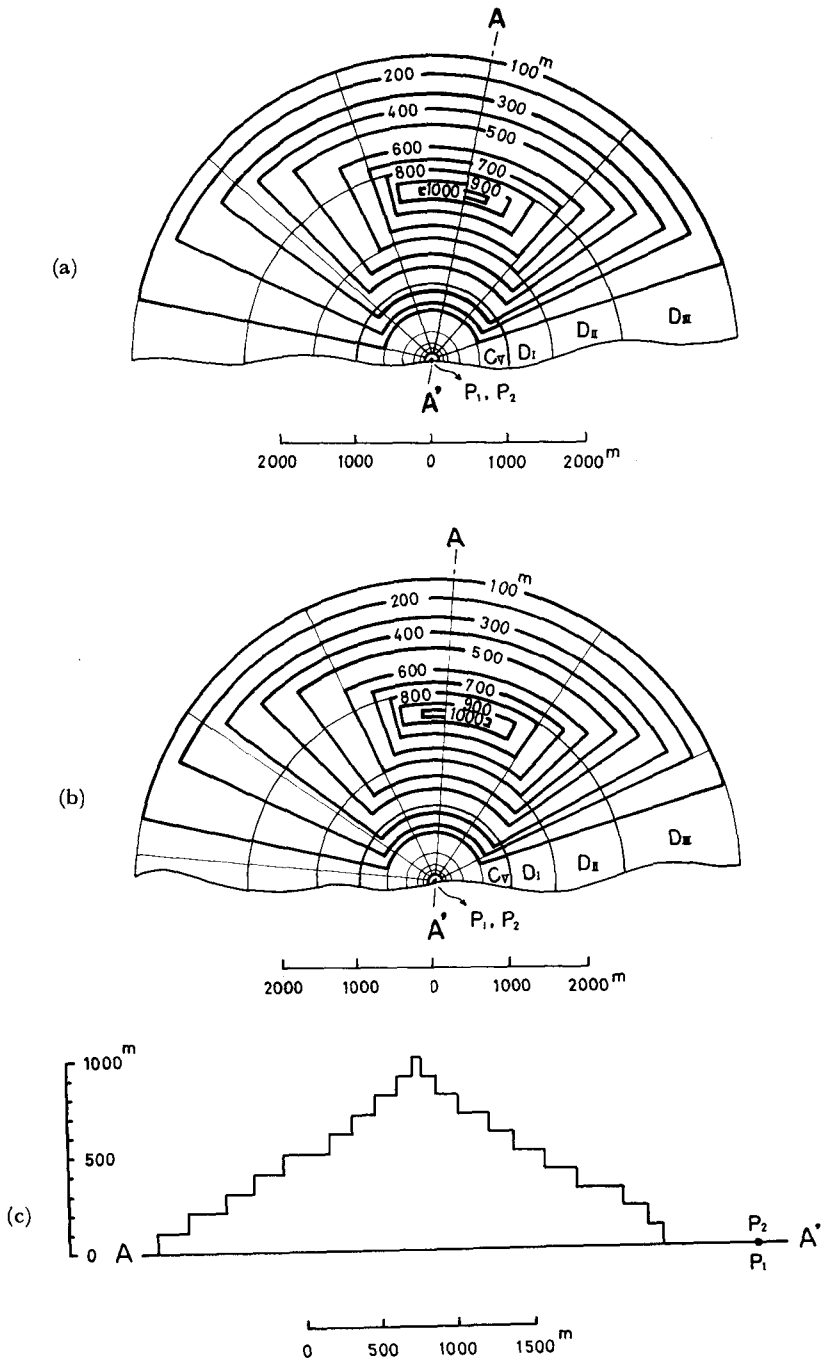


Fig. 6.

**§6. The value of the topographic effect  $\Gamma = \Sigma_m = \Gamma \Sigma(f_m \cdot \sigma)$  as compared with its exact value by employing a model topography**

A model topography employed here is a pile of lots of sectorial blocks of equal thickness of 100 m forming a pyramid (Figs. 6(a), 6(b) and 6(c)). The lowest block standing on the datum level through a gravity station  $P_1$  at the ground surface is just covered by the continuous zones  $C_V$ ,  $D_I$ ,  $D_{II}$  and  $D_{III}$ , where  $C_V$ , e.g., means the subzone V of the zone C, and two radial lines separated by  $150^\circ$ . Another station  $P_2$  situated 5 m ( $= -\delta z$ ) vertically above  $P_1$  is employed for an examination of the topographic effect on the vertical gradient of gravity at  $P_1$  as compared with its exact value. Assuming  $2.67 \text{ gm/cm}^3$  to the density  $\sigma$ , the exact values of the topographical effects at  $P_1$  and  $P_2$ , being denoted by  $\Gamma_{(1)}$  and  $\Gamma_{(2)}$  respectively, can be computed by making use of the Eq. (10). For tabular computation of  $\Gamma_{(1)}$  and  $\Gamma_{(2)}$  by tables I-1, 2, ..., 5 and  $\sigma = 2.67 \text{ gm/cm}^3$ , a transparent graticule has been prepared upon which the necessary concentric circles and radial lines are drawn, with a scale equal to the scale of the maps to be used, to show the compartments. The value of  $\Gamma_{(2)}$  obtained by the tabular computation means that the empty space between the ground surface and the datum level passing through  $P_2$  is filled with mass of density  $\sigma$ , so that the vertically downward attraction of an infinitely broad, horizontal plate of a thickness  $\delta z (= 5.00 \text{ m})$  and of the density  $\sigma$ ,  $0.04193 \cdot \delta z \cdot \sigma \text{ mgal}$ , should be subtracted from the values  $\Gamma_{(2)}$ , because for both the points the topographical mass lying above the datum level through the ground station should be removed. Let  $\Gamma'_{(2)}$  denote the value of  $\Gamma_{(2)}$  subjected to the above subtraction. In Figs. 6(a) and 6(b) one of the radial lines passes through a point shifted to the right and left sides respectively of the middle point of the summit line of the pyramid. The comparisons between the tabular and exact values of  $\Gamma_{(1)}$  and  $\Gamma'_{(2)}$  are shown in Table II and III.

The above two means, 0.089 and 0.095 mgal, of the corrections to be added to the tabular values are nearly 0.1 mgal which is 10 times the sensitivity of the present portable gravimeter, 0.01 mgal. In this model the corrections are

Table II. Topographical effect  $\Gamma_{(1)} = \Sigma(\Gamma_m)_{(1)}$  upon the intensity of gravity  $g_1$  at a ground station  $P_1$  with  $\sigma = 2.67 \text{ gm/cm}^3$ .

	Fig. 6(a)	Fig. 6(b)	Mean
	mgal	mgal	mgal
Tabular value	-3.167	-3.210	-3.184
Exact value	-3.273	-3.273	-3.273
Corr. to be added to the tabular value	-0.106	-0.072	-0.089

Table III. Topographical effect  $\Gamma'_{(2)} = \Sigma(\Gamma_m)_{(2)} - 0.04193 \cdot \delta z \cdot \sigma$  upon the intensity of gravity  $g_2$  at a free-air station  $P_2$  with  $\sigma = 2.67$  gm/cm<sup>3</sup>.

	Fig. 6(a)	Fig. 6(b)	Mean
	mgal	mgal	mgal
Tabular value	-3.087	-3.121	-3.104
Exact value	-3.199	-3.199	-3.199
Corr. to be added to the tabular value	-0.112	-0.078	-0.095

negative, but another model may be possible which produces positive correction. Consequently, with the actual topography within a distance of some tens of kilometers or 100 km from a gravity station, the correction to be added to the tabular value due to the total topography would not take a very large value, and it may be expected that the reliability of Tables I-1, 2, ..., 5 for the total, actual topography would be at least  $\pm 0.1$  mgal. However, examination of this reliability on more rigorous and reasonable basis is a task the author has to undertake.

In Table IV are shown the comparisons between the tabular and exact values of  $(\Gamma_{(1)} - \Gamma'_{(2)})/5.00$ , i.e., the topographical effect in mgal/m upon the intensity of the vertical gradient of gravity at the ground station  $P_1$  which is obtained by  $(g_1 - g_2)/\delta z$  (cf. the Eq. (13)). The sensitivity of the gravimeter to

Table IV. Topographical effect  $(\Gamma_{(1)} - \Gamma'_{(2)})/5.00$  upon the intensity of vertical gradient of gravity at the ground station  $P_1$ .

	Fig. 6(a)	Fig. 6(b)	Mean
	mgal/m	mgal/m	mgal/m
Tabular value	-0.0160	-0.0160	-0.0160
Exact value	-0.0148	-0.0148	-0.0148
Corr. to be added to the tabular value	+0.0012	+0.0012	+0.0012

measure  $g_1$  and  $g_2$  is 0.01 mgal, and therefore, the sensitivity of it as a vertical gradiometer of gravity with  $\delta z = 5.00$  m is  $0.01\sqrt{2}/5.00 = 0.0028$  mgal/m, which is nearly twice or in the same order of magnitude of the value 0.0012 mgal/m, the mean of the two corrections to be added to the tabular values in the table. This is just opposite to the case in which the error involved in the tabular value of the topographic correction upon gravity value is, already mentioned, about 10 times as large as the sensitivity of the gravimeter. This result indicates that Tables I-1, 2, ..., 5 are more reliable for the vertical gradient of gravity than for gravity.

**§7. Some examples of the topographic corrections for gravity and its vertical gradient**

From November 1958 to October 1959, the vertical gradients of gravity were measured at 145 stations occupied at the first order bench marks in the central part of Honshû, Japan, by using a Worden gravimeter No. 127 of the scale constant=0.1004 mgal per small dial division and a jeep equipped with an extensible ladder of which the top plate to mount the gravimeter when fully extended is at a height of about 5 m above the ground surface; this height changed from 4.85 to 5.25 m according to the station. At the four stations selected from the above 145 stations, the topographic corrections were carried out by Tables I-1, 2, ..., 5 upon the intensities of gravity and its vertical gradients at these four stations to obtain their Modified Bouguer anomalies at sea-level. The results are shown in Table V. In the table Simple Bouguer anomaly, a name given to  $\Delta g_0''$ , is identical with Bouguer anomaly employed in the pendulum age of the gravity measurement; in this old age the topographic correction was disregarded with usual topography owing to a low accuracy of the gravity measurement and further the free-air reduction was made by the coefficient 0.3086 mgal/m, the vertical gradient of the normal gravity near the sea-level. In the present age of a high precision gravimeter, the topographic corrections are requisite to the observed values not only of gravity and but also its vertical gradient, the latter being not observed in

Table V. Actual examples of the topographic corrections for gravity and its vertical gradient.

Station No.	Bench mark No.	Height above sea-level H	Simple Bouguer anomaly at $P_1$ $\Delta g_0''$	Observed value of vertical gradient of gravity $(g_1 - g_2) / \delta z$
		m	mgal	mgal/m
14	644	851	-31.4 *	0.265
32	813	201	-12.8 *	0.252
43	5191	106	+ 0.4 *	0.268
58	863	17	+16.2 *	0.297

Table V (cont.).

Station No.	Topographic effect upon $g_1$ $\Gamma_{(1)}$	Modified Bouguer anomaly with a distance of 25 km $\Delta g_0'' - \Gamma_{(1)} \equiv \Delta g_0''^{(25)}$	Topographic effect on the gradient $(\Gamma_{(1)} - \Gamma'_{(2)}) / \delta z$	Vertical gradient at $P_1$ corrected for topography $\partial g'' / \partial z$
	mgal	mgal	mgal/m	mgal/m
14	- 4.9	-26.5	-0.013	0.278
32	-10.6	- 2.2	-0.041	0.293
43	- 2.7	+ 3.1	-0.045	0.313
58	- 0.4	+16.6	-0.010	0.307



Table V (cont.).

Station No.	Anomalies in $\partial g''/\partial z$	Corr. to the usual free-air reduction	Modified Bouguer anomaly corrected for $\lambda H$	$\Delta g_0'' - \Delta g_0''^{(25)}$	$\Delta g_0''^{(25)} - \Delta g_0''^{(25)}$
	$\partial g''/\partial z - 0.309 = \lambda$	$\lambda H$	$\Delta g_0''^{(25)}$		
	mgal/m	mgal	mgal	mgal	mgal
14	-0.031	-26.4	-52.9	+21.5	+26.4
32	-0.016	-3.2	-5.4	-7.4	+3.2
43	+0.004	+0.4	+3.5	-3.1	-0.4
58	-0.002	0.0	+16.6	-0.4	0.0

\* Tsuboi *et al.* (1955)

the pendulum age. Modified Bouguer anomaly means Simple Bouguer anomaly upon which the topographic correction was done for the topography within a certain distance from the gravity station. The figure 25 in the upper suffix <sup>(25)</sup> of the sign of Modified Bouguer anomaly indicates the distance in km from the gravity station within which the topographic correction has been done. This upper suffix, of which inside the brackets the figure of any desired distance is written, is what N. Kumagai has been using in his unpublished works, and is employed in this paper by his permission. The lower suffix <sub>0</sub> attached to Modified Bouguer anomaly corrected for  $\lambda H$ ,  $\Delta g_0''^{(25)}$ , indicates that it is Modified Bouguer anomaly *at sea-level*, in contrast to which  $\Delta g_0''^{(25)}$  is Modified Bouguer anomaly *at a station in free-air*. These two kinds of phrase "at sea-level" and "at a station in free-air" were already employed by N. Kumagai, *et al.* (1960). Of the three kinds of Bouguer anomalies, namely Simple Bouguer anomaly,  $\Delta g_0''$ , Modified one,  $\Delta g_0''^{(25)}$ , and Modified one corrected for  $\lambda H$ ,  $\Delta g_0''^{(25)}$ , the most trustful one is the last mentioned one.

The errors of the above mentioned first and second Bouguer anomalies against the third are shown under the headings  $\Delta g_0'' - \Delta g_0''^{(25)}$  and  $\Delta g_0''^{(25)} - \Delta g_0''^{(25)}$  in the last two columns of Table V (cont.), indicating that the error generally increases as the height of the station increases. Therefore, it can be said that both the two anomalies  $\Delta g_0''$  and  $\Delta g_0''^{(25)}$  in a lofty mountainous area can never be used for finding the state of the isostatic equilibrium, or generally speaking, of the mass distribution under the area and, instead, the Modified Bouguer anomalies  $\Delta g_0''^{(S)}$  should be used, of which *S* in the brackets of the upper suffix indicates the greatest distance within which the topographic effect has been removed.

### §8. Method of correction for near topography assumed two-dimensional

Near the gravity station frequently appear the topographies of ascending and

descending steps which may be treated as two-dimensional with the cross-section as shown in Fig. 7(a) and 7(b). In the figures  $H$  and  $H'$  are positive quantities and the axis of  $Z$  is directed vertically downward. This kind of correction may be made, as usually done by condensation of the excess or defect of mass respectively above or below the ground level  $LL'$  upon a horizontal plane (shown by a broken line in Fig. 7(a) and 7(b)) which divides the excess or defect of mass into two equal

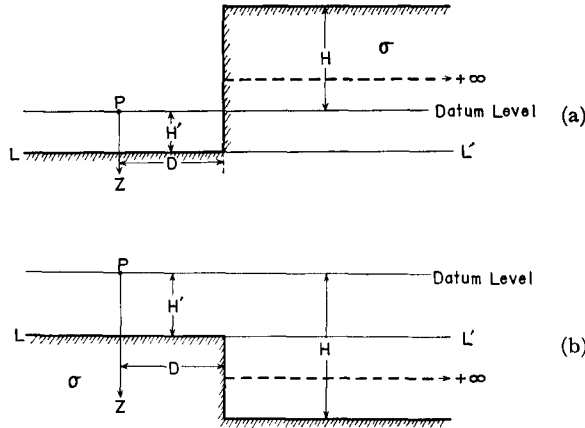


Fig. 7.

parts and by calculating the effect of such a condensed mass at the gravity station  $P$ . In this case, the larger is the ratio  $H/D$ , the larger becomes the error of the condensation. If the vertical attraction at  $P$  of the mass of the ascending step (Fig. 7(a)) above the ground level  $LL'$  is denoted by  $F$ , we have

$$F = -2\gamma \cdot \sigma \cdot \left\{ \frac{\pi}{2} (H - H') + D \ln \frac{\sqrt{D^2 + H'^2}}{\sqrt{D^2 + H^2}} - H \tan^{-1} \frac{D}{H} + H' \tan^{-1} \frac{D}{H'} \right\}, \dots (19)$$

which can be rewritten as follows:

$$F = -\gamma \cdot \sigma \cdot D \cdot \left\{ \pi \frac{H - H'}{D} + \ln \frac{1 + (H'/D)^2}{1 + (H/D)^2} - 2 \frac{H}{D} \tan^{-1} \frac{D}{H} + 2 \frac{H'}{D} \tan^{-1} \frac{D}{H'} \right\}. \dots (20)$$

Further putting

$$q = -\gamma \cdot \left\{ \pi \left( \frac{H}{D} - \frac{H'}{D} \right) + \ln \frac{1 + (H'/D)^2}{1 + (H/D)^2} - 2 \frac{H}{D} \cot^{-1} \frac{H}{D} + 2 \frac{H'}{D} \cot^{-1} \frac{H'}{D} \right\}, \dots (21)$$

we get for both the excess and defect masses

$$F = q \cdot \sigma \cdot D. \dots (22)$$

In Tables VI-1 and 2 attached in the end of this paper are shown the values of  $-q$  in  $\mu\text{gal per gm}\cdot\text{cm}^{-3}$  per m for every 0.05 of  $H'/D$  from 0.00 to 5.00 and of  $H/D$  from 0.05 to 5.00. The tabular values of  $-q$  for high values of  $H'/D$  are useful for the measurements of the vertical gradient of gravity in which the upper station  $P_2$  is situated at a height  $\delta z$  above the ground surface, which changes around 5.00 m according to station. In the tables the values of  $-q$  are calculated for  $H \geq H'$ , i.e.,  $H/D \geq H'/D$ . If  $H < H'$ , i.e.,  $H/D < H'/D$ , the tabular values of  $-q$  can be used by simply changing the minus sign with the plus. After the topographical correction is finished by these tables, the ground surface around the station takes a horizontal plane extending to the distance beyond which the distant topographical corrections are to be done by using Tables I-1, ..., 5. The height  $H'$  of the gravity station above this horizontal ground surface depends on the height of the stand on which the gravimeter is mounted. In order that the near topographical correction is consistent with the distant one, the free-air space between the above mentioned horizontal ground surface and the datum level through  $P$  should be filled with mass of density  $\sigma$ , that is, the attraction of  $2\pi\gamma\cdot\sigma\cdot H'$  should be added to the station  $P$ . In case of the measurement of vertical gradient of gravity, the similar treatment should be done for both the two points  $P_1$  and  $P_2$ .

When the step is descending (Fig. 7(b)) the same equation as the Eq. (12) and the addition of the attraction  $2\pi\gamma\cdot\sigma\cdot H'$  to the station  $P$  hold true. When the near topography is a bank or a ditch, of which the width is  $l$  and the horizontal distances of the edges from  $P$  are  $D$  and  $D+l$ , the effect of the bank or ditch is  $F_{(D)} - F_{(D+l)}$ , where  $F_{(D)}$  is the Eq. (20) and  $F_{(D+l)}$  is the same equation in which  $D$  is replaced by  $D+l$ .

### Acknowledgement

The author wishes to express his deep gratitude to Professor Emeritus N. Kumagai for the suggestion of this investigation and a constant encouragement throughout this work. Thanks are also due to Dr. S. Nishimura for his assistance in laborous computations.

### Reference

- BOWIE, W. (1917): Investigations of Gravity and Isostasy. *U.S. Coast and Geod. Surv., Spec. Publ.*, **40**, pp. 9-18.
- BULLARD, E.C. (1936): Gravity Measurements in East Africa. *Phil. Trans. Roy. Soc. London*, **A235**, pp. 486-491.
- FUCHIDA, T. (1948): Topographic Corrections for Gravimeter Stations. *Geophysical Exploration* **1**(1), pp. 14-21. (in Japanese)
- HAYFORD, J.F. and W. BOWIE (1912): The Effect of Topography and Isostatic Compensation upon the Intensity of Gravity. *U.S. Coast and Geod. Surv., Spec. Publ.*, **10**, pp. 13-53.

- HAMMER, S. (1939): Terrain Correction for Gravimeter Stations. *Geophysics*, **4**(3), pp. 184–194.
- JUNG, K. (1927): Diagramme zur Bestimmung der Terrainwirkung für Pendel und Drehwage und zur Bestimmung der Wirkung „Zweidimensionaler“ Massenarrangements. *Z. Geophysik*, **3**(5), pp. 201–212.
- KUMAGAI, N., E. ABE and Y. YOSHIMURA (1960): Measurement of Vertical Gradient of Gravity and its Significance. *Boll. Geof. teor. ed appl.*, **11**(8), pp. 613–614.
- MATSUDA, T. (1952): Correction Tables for Gravitational Exploration. *Geol. Surv. Japan, Spec. Publ.*, pp. 1–106. (in Japanese)
- TSUBOI, C., A. JITSUKAWA and H. TAJIMA (1955): Gravity Survey along the Lines of Precise Levels throughout Japan by Means of a Worden Gravimeter, Part VI, Chûbu District. *Bull. Earthq. Res. Inst., Suppl. IV*, Part V, pp. 278–300.



Table I-2. Topographic effect of one compartment of the subzone II upon the intensity of gravity.  
 $-f_{II}$  in  $\mu\text{gal}$  for  $\sigma=1.00\text{ gm}\cdot\text{cm}^{-3}$

(a)						(b)					
lh-Hl m	00	20	40	60	80	lh-Hl m	00	20	40	60	80
ABCDE	ABCDE	ABCDE	ABCDE	ABCDE	ABCDE	ABCDE	ABCDE	ABCDE	ABCDE	ABCDE	ABCDE
	0.0	0.0	0.1	0.2	0.3						
100	0.4	0.6	0.8	1.0	1.3	5100	1005.7	1013.2	1020.6	1028.2	1035.8
200	1.6	2.0	2.4	2.8	3.2	5200	1043.4	1051.1	1058.8	1066.5	1074.2
300	3.7	4.2	4.7	5.2	5.8	5300	1081.9	1089.7	1097.5	1105.2	1113.0
400	6.4	7.1	7.8	8.6	9.4	5400	1120.9	1128.8	1136.7	1144.5	1152.3
500	10.2	11.0	11.9	12.8	13.7	5500	1160.2	1168.3	1176.4	1184.4	1192.4
600	14.6	15.6	16.6	17.7	18.8	5600	1200.4	1208.5	1216.6	1224.8	1232.9
700	20.0	21.1	22.2	23.4	24.7	5700	1241.0	1249.3	1257.5	1265.6	1273.8
800	26.0	27.3	28.7	30.0	31.4	5800	1282.0	1290.4	1298.7	1307.1	1315.5
900	32.9	34.4	35.9	37.4	39.0	5900	1323.9	1332.3	1340.8	1349.3	1357.7
1000	40.6	42.3	44.0	45.6	47.3	6000	1366.2	1374.8	1383.3	1391.9	1400.5
1100	49.0	50.8	52.6	54.5	56.4	6100	1409.0	1417.6	1426.3	1435.0	1443.7
1200	58.4	60.4	62.4	64.4	66.4	6200	1452.5	1461.1	1469.9	1478.8	1487.5
1300	68.5	70.6	72.7	74.9	77.2	6300	1496.2	1505.0	1513.7	1522.6	1531.5
1400	79.5	81.7	84.0	86.3	88.7	6400	1540.4	1549.3	1558.2	1567.2	1576.3
1500	91.1	93.5	96.0	98.5	101.0	6500	1585.3	1594.2	1603.2	1612.3	1621.4
1600	103.6	106.2	108.8	111.4	114.1	6600	1630.6	1639.6	1648.7	1657.9	1667.2
1700	116.8	119.6	122.4	125.3	128.1	6700	1676.4	1685.6	1694.8	1704.0	1713.3
1800	130.9	133.8	136.7	139.7	142.7	6800	1722.6	1731.9	1741.1	1750.4	1759.8
1900	145.7	148.8	151.9	155.0	158.2	6900	1769.2	1778.6	1788.0	1797.4	1806.9
2000	161.4	164.5	167.7	171.0	174.3	7000	1816.5	1826.0	1835.5	1845.0	1854.6
2100	177.7	181.1	184.5	188.0	191.5	7100	1864.2	1873.7	1883.2	1892.7	1902.3
2200	194.9	198.4	202.0	205.6	209.2	7200	1911.9	1921.7	1931.4	1941.1	1950.7
2300	212.9	216.7	220.4	224.1	227.8	7300	1960.4	1970.3	1980.2	1990.0	1999.8
2400	231.6	235.4	239.2	243.0	247.1	7400	2009.6	2019.4	2029.2	2039.0	2048.8
2500	251.1	255.1	259.0	263.0	267.0	7500	2058.6	2068.5	2078.5	2088.5	2098.5
2600	271.2	275.4	279.6	283.8	288.0	7600	2108.4	2118.4	2128.4	2138.4	2148.5
2700	292.3	296.5	300.8	305.1	309.5	7700	2158.5	2168.7	2178.9	2188.9	2199.0
2800	313.9	318.3	322.7	327.2	331.7	7800	2209.1	2219.2	2229.4	2239.5	2249.6
2900	336.2	340.8	345.5	350.2	354.8	7900	2259.9	2270.2	2280.5		
3000	359.5	364.3	369.1	373.9	378.6	8000					
3100	383.4	388.3	393.2	398.1	403.1						
3200	408.2	413.2	418.2	423.2	428.2						
3300	433.4	438.7	443.9	449.1	454.3						
3400	459.5	464.8	470.2	475.6	481.0						
3500	486.3	491.7	497.2	502.7	508.2						
3600	513.7	519.3	524.9	530.6	536.3						
3700	542.0	547.7	553.4	559.2	565.0						
3800	570.8	576.6	582.5	588.5	594.5						
3900	600.4	606.3	612.3	618.4	624.4						
4000	630.4	636.5	642.7	649.0	655.3						
4100	661.5	667.7	673.9	680.3	686.7						
4200	693.0	699.4	705.8	712.3	718.8						
4300	725.3	731.8	738.4	745.0	751.6						
4400	758.2	764.8	771.4	778.0	784.7						
4500	791.4	798.2	805.1	812.0	819.0						
4600	825.8	832.6	839.5	846.5	853.5						
4700	860.5	867.5	874.5	881.6	888.7						
4800	895.8	902.9	910.0	917.2	924.5						
4900	931.8	939.1	946.3	953.6	961.0						
5000	968.4	975.8	983.3	990.7	998.2						

Table I-3. Topographic effect of one compartment of the subzone III upon the intensity of gravity.  
 $-f_{III}$  in  $\mu\text{gal}$  for  $\sigma=1.00 \text{ gm}\cdot\text{cm}^{-3}$

(a)					(b)					(c)				
lh-Hl m	00	25	50	75	lh-Hl m	00	25	50	75	lh-Hl m	00	25	50	75
ABCDE	ABCDE	ABCDE	ABCDE	ABCDE	ABCDE	ABCDE	ABCDE	ABCDE	ABCDE	ABCDE	ABCDE	ABCDE	ABCDE	ABCDE
100	0.0	0.0	0.1	0.1	5100	654.0	660.3	666.7	673.0	10100	2422.2	2433.3	2444.5	2455.7
200	0.3	0.4	0.6	0.8	5200	679.3	685.7	692.1	698.6	10200	2466.9	2478.1	2489.4	2500.6
300	1.0	1.3	1.6	1.9	5300	705.1	711.7	718.3	724.9	10300	2511.8	2523.1	2534.4	2545.7
400	2.3	2.7	3.2	3.6	5400	731.4	738.0	744.6	751.3	10400	2557.1	2568.4	2579.7	2591.0
500	4.1	4.7	5.2	5.8	5500	758.0	764.8	771.6	778.3	10500	2602.4	2613.9	2625.3	2636.9
600	6.4	7.0	7.7	8.5	5600	785.1	792.0	798.9	805.8	10600	2648.4	2659.9	2671.5	2683.0
700	9.2	10.0	10.8	11.7	5700	812.7	819.7	826.8	833.9	10700	2694.5	2706.0	2717.7	2729.3
800	12.6	13.5	14.4	15.4	5800	840.9	847.9	855.0	862.0	10800	2740.9	2752.5	2764.2	2775.8
900	16.4	17.5	18.6	19.7	5900	869.0	876.2	883.5	890.8	10900	2787.4	2799.0	2810.8	2822.7
1000	20.8	21.9	23.1	24.3	6000	898.0	905.3	912.6	920.0	11000	2834.5	2846.3	2858.1	2869.9
1100	25.5	26.8	28.2	29.6	6100	927.3	934.7	942.2	949.8	11100	2881.6	2893.3	2905.2	2917.2
1200	31.0	32.4	33.8	35.3	6200	957.3	964.8	972.3	979.8	11200	2929.2	2941.2	2953.1	2965.0
1300	36.9	38.4	40.0	41.7	6300	987.4	995.0	1002.6	1010.2	11300	2977.0	2988.9	3000.8	3012.8
1400	43.4	45.1	46.8	48.5	6400	1018.0	1025.8	1033.5	1041.2	11400	3024.9	3037.1	3049.3	3061.5
1500	50.2	52.0	53.8	55.7	6500	1049.0	1056.9	1064.8	1072.6	11500	3073.7	3085.8	3097.9	3110.0
1600	57.6	59.6	61.6	63.5	6600	1080.5	1088.4	1096.3	1104.2	11600	3122.1	3134.2	3146.4	3158.6
1700	65.5	67.6	69.7	71.9	6700	1112.2	1120.2	1128.2	1136.4	11700	3170.8	3183.0	3195.2	3207.5
1800	74.0	76.2	78.4	80.7	6800	1144.6	1152.8	1160.9	1169.1	11800	3219.8	3232.1	3244.5	3257.0
1900	82.9	85.2	87.5	89.9	6900	1177.2	1185.3	1193.5	1201.8	11900	3269.5	3282.0	3294.4	3306.8
2000	92.4	94.8	97.3	99.8	7000	1210.2	1218.6	1227.0	1235.5	12000	3319.2	3331.6	3344.1	3356.6
2100	102.3	104.8	107.4	110.0	7100	1243.9	1252.3	1260.8	1269.3	12100	3369.1	3381.6	3394.0	3406.4
2200	112.7	115.5	118.3	121.0	7200	1277.7	1286.2	1294.8	1303.5	12200	3419.0	3431.6	3444.2	3456.8
2300	123.7	126.5	129.4	132.2	7300	1312.2	1320.7	1329.2	1337.9	12300	3469.4	3482.1	3494.8	3507.4
2400	135.2	138.2	141.2	144.1	7400	1346.7	1355.5	1364.2	1372.9	12400	3520.0	3532.6	3545.3	3558.1
2500	147.2	150.2	153.3	156.4	7500	1381.7	1390.4	1399.3	1408.3	12500	3570.9	3583.7	3596.8	3609.8
2600	159.6	162.8	166.1	169.4	7600	1417.3	1426.2	1435.2	1444.2					
2700	172.6	175.9	179.2	182.6	7700	1453.2	1462.1	1471.1	1480.1					
2800	186.0	189.5	193.0	196.5	7800	1489.3	1498.5	1507.7	1516.8					
2900	200.1	203.6	207.2	210.7	7900	1525.9	1535.0	1544.2	1553.4					
3000	214.3	218.0	221.8	225.6	8000	1562.7	1572.1	1581.5	1590.9					
3100	229.3	233.1	236.9	240.7	8100	1600.4	1609.9	1619.2	1628.7					
3200	244.6	248.6	252.6	256.6	8200	1638.2	1647.6	1657.0	1666.6					
3300	260.7	264.8	268.9	273.0	8300	1676.3	1685.9	1695.4	1704.9					
3400	277.1	281.2	285.4	289.7	8400	1714.4	1724.0	1733.8	1743.6					
3500	294.0	298.3	302.6	307.0	8500	1753.4	1763.2	1773.0	1782.8					
3600	311.3	315.7	320.2	324.7	8600	1792.6	1802.5	1812.4	1822.4					
3700	329.2	333.7	338.3	342.9	8700	1832.3	1842.2	1852.2	1862.2					
3800	347.6	352.3	356.9	361.6	8800	1872.2	1882.2	1892.2	1902.2					
3900	366.3	371.1	376.0	380.9	8900	1912.3	1922.6	1932.9	1943.1					
4000	385.7	390.6	395.5	400.4	9000	1953.2	1963.4	1973.7	1983.9					
4100	405.3	410.3	415.4	420.6	9100	1994.1	2004.4	2014.8	2025.3					
4200	425.8	430.9	436.0	441.2	9200	2035.7	2046.0	2056.3	2066.7					
4300	446.4	451.7	457.0	462.3	9300	2077.2	2087.7	2098.2	2108.7					
4400	467.6	473.0	478.4	483.8	9400	2119.2	2129.6	2140.0	2150.6					
4500	489.2	494.7	500.2	505.8	9500	2161.4	2172.2	2183.0	2193.7					
4600	511.4	517.0	522.6	528.3	9600	2204.3	2214.9	2225.6	2236.3					
4700	534.0	539.7	545.4	551.1	9700	2247.0	2257.7	2268.6	2279.6					
4800	556.8	562.8	568.8	574.7	9800	2290.5	2301.4	2312.3	2323.2					
4900	580.6	586.6	592.6	598.7	9900	2334.1	2345.0	2356.0	2367.0					
5000	604.7	610.7	616.8	622.9	10000	2378.0	2389.0	2400.0	2411.0					

Table I-4. Topographic effect of one compartment of the subzone IV upon the intensity of gravity.  
 $-f_{IV}$  in  $\mu\text{gal}$  for  $\sigma=1.00\text{ gm}\cdot\text{cm}^{-3}$

(a)			(b)			(c)			(d)		
lh-Hl <sub>m</sub>	00	50	lh-Hl <sub>m</sub>	00	50	lh-Hl <sub>m</sub>	00	50	lh-Hl <sub>m</sub>	00	50
ABCDE	ABCDE	ABCDE	ABCDE	ABCDE	ABCDE	ABCDE	ABCDE	ABCDE	ABCDE	ABCDE	ABCDE
	0.0	0.0									
100	0.2	0.4	5100	417.7	425.9	10100	1600.2	1615.5	15100	3444.4	3465.6
200	0.6	1.0	5200	434.2	442.5	10200	1630.9	1646.4	15200	3486.9	3508.3
300	1.5	2.0	5300	450.8	459.3	10300	1662.0	1677.5	15300	3529.8	3551.4
400	2.6	3.2	5400	467.9	476.4	10400	1693.2	1709.0	15400	3573.0	3594.6
500	4.0	4.9	5500	485.0	493.8	10500	1725.0	1740.9	15500	3616.4	3638.1
600	5.8	6.9	5600	502.7	511.8	10600	1757.0	1773.1	15600	3659.8	3681.6
700	8.0	9.2	5700	520.8	529.8	10700	1789.2	1805.2	15700	3703.5	3725.4
800	10.4	11.8	5800	539.0	548.3	10800	1821.4	1837.7	15800	3747.5	3769.5
900	13.2	14.6	5900	557.6	566.9	10900	1854.0	1870.4	15900	3791.6	3813.7
1000	16.2	17.8	6000	576.4	586.0	11000	1886.9	1903.5	16000	3835.8	3858.0
1100	19.6	21.4	6100	595.6	605.2	11100	1920.2	1936.8	16100	3880.3	3902.6
1200	23.4	25.3	6200	615.0	624.9	11200	1953.6	1970.4	16200	3925.0	3947.5
1300	27.4	29.5	6300	634.9	644.8	11300	1987.3	2004.2	16300	3970.0	3992.6
1400	31.7	34.0	6400	654.7	664.9	11400	2021.3	2038.4	16400	4015.1	4037.7
1500	36.4	38.8	6500	675.2	685.5	11500	2055.5	2072.5	16500	4060.4	4083.1
1600	41.4	44.0	6600	695.8	706.2	11600	2089.7	2107.0	16600	4105.9	4128.7
1700	46.7	49.5	6700	716.7	727.3	11700	2124.4	2141.9	16700	4151.6	4174.1
1800	52.4	55.3	6800	737.9	748.7	11800	2159.4	2177.0	16800	4197.3	4220.3
1900	58.4	61.5	6900	759.5	770.4	11900	2194.6	2212.3	16900	4243.3	4266.4
2000	64.7	68.0	7000	781.3	792.3	12000	2230.0	2247.8	17000	4289.6	4312.7
2100	71.4	74.8	7100	803.5	814.6	12100	2265.7	2283.7	17100	4335.9	4359.2
2200	78.3	81.8	7200	825.8	837.1	12200	2301.6	2319.6	17200	4382.6	4406.0
2300	85.5	89.2	7300	848.5	860.0	12300	2337.7	2355.9	17300	4429.4	4452.9
2400	93.1	97.0	7400	871.6	883.2	12400	2374.2	2392.5	17400	4476.4	4499.8
2500	101.0	105.1	7500	894.8	906.6	12500	2410.9	2429.3	17500	4523.4	4547.1
2600	109.2	113.4	7600	918.4	930.4	12600	2447.8	2466.3	17600	4570.8	4594.5
2700	117.7	122.1	7700	942.4	954.5	12700	2484.9	2503.6	17700	4618.2	4642.0
2800	126.6	131.2	7800	966.6	978.7	12800	2522.3	2541.1	17800	4665.9	4689.8
2900	135.9	140.5	7900	990.9	1003.3	12900	2559.9	2578.8	17900	4713.8	4737.8
3000	145.3	150.2	8000	1015.7	1028.2	13000	2597.7	2616.8	18000	4761.9	4785.9
3100	155.1	160.1	8100	1040.7	1053.2	13100	2635.8	2654.9	18100	4809.9	4834.1
3200	165.2	170.4	8200	1065.9	1078.7	13200	2674.1	2693.3	18200	4858.3	4882.5
3300	175.7	181.1	8300	1091.6	1104.6	13300	2712.6	2731.9	18300	4906.8	4931.2
3400	186.5	192.0	8400	1117.6	1130.6	13400	2751.4	2770.9	18400	4955.5	4979.9
3500	197.6	203.3	8500	1143.7	1156.9	13500	2790.3	2809.9	18500	5004.3	5028.9
3600	209.0	214.8	8600	1170.0	1183.3	13600	2829.5	2849.2	18600	5053.4	5078.0
3700	220.7	226.7	8700	1196.8	1210.3	13700	2868.9	2888.8	18700	5102.6	5127.2
3800	232.7	238.8	8800	1223.9	1237.4	13800	2908.7	2928.6	18800	5151.9	5176.6
3900	245.1	251.4	8900	1251.0	1264.8	13900	2948.5	2968.5	18900	5201.4	5226.2
4000	257.8	264.2	9000	1278.8	1292.7	14000	2988.7	3008.9	19000	5251.2	5276.1
4100	270.7	277.3	9100	1306.6	1320.7	14100	3029.0	3049.2	19100	5301.0	5325.9
4200	284.1	290.8	9200	1334.8	1348.9	14200	3069.5	3089.9	19200	5350.8	5375.9
4300	297.6	304.5	9300	1363.0	1377.2	14300	3110.4	3130.9	19300	5401.0	5426.1
4400	311.6	318.7	9400	1391.6	1406.1	14400	3151.3	3171.9	19400	5451.3	5476.5
4500	325.8	333.0	9500	1420.6	1435.2	14500	3192.5	3213.2	19500	5501.8	5527.1
4600	340.4	347.8	9600	1449.9	1464.7	14600	3234.0	3254.9	19600	5552.5	5577.7
4700	355.2	362.8	9700	1479.4	1494.2	14700	3275.7	3296.5	19700	5603.1	5628.4
4800	370.5	378.1	9800	1509.2	1524.2	14800	3317.4	3338.5	19800	5653.9	5679.5
4900	385.8	393.7	9900	1539.2	1554.2	14900	3359.5	3380.6	19900	5705.1	
5000	401.7	409.7	10000	1569.4	1584.8	15000	3401.8	3423.1			



Table I-5. Topographic effect of one compartment of the subzone V upon the intensity of gravity.  
 $-f_V$  in  $\mu\text{gal}$  for  $\sigma=1.00 \text{ gm}\cdot\text{cm}^{-3}$

(a)			(b)			(c)			(d)			(e)			(f)			(g)			
lh-Hl m	00	50	lh-Hl m	00	50	lh-Hl m	00	50	lh-Hl m	00	50	lh-Hl m	00	50	lh-Hl m	00	50	lh-Hl m	00	50	
ABCDE	ABCDE	ABCDE	ABCDE	ABCDE	ABCDE	ABCDE	ABCDE	ABCDE	ABCDE	ABCDE	ABCDE	ABCDE	ABCDE	ABCDE	ABCDE	ABCDE	ABCDE	ABCDE	ABCDE	ABCDE	ABCDE
100	0.0	0.0	5100	264.8	270.0	10100	1029.0	1039.1	15100	2264.4	2279.0	20100	3927.8	3946.2	25100	5965.0	5987.1	30100	8316.0	8340.7	
200	0.1	0.2	5200	275.2	280.6	10200	1049.2	1059.2	15200	2293.6	2308.4	20200	3964.8	3983.4	25200	6009.4	6031.7	30200	8365.5	8390.4	
300	0.4	0.7	5300	286.0	291.4	10300	1069.5	1079.8	15300	2323.0	2337.8	20300	4002.2	4021.2	25300	6053.8	6075.9	30300	8415.5	8440.6	
400	0.9	1.3	5400	296.8	302.4	10400	1090.2	1100.6	15400	2352.6	2367.5	20400	4040.1	4058.9	25400	6098.1	6120.2	30400	8465.6	8490.6	
500	1.7	2.1	5500	308.0	313.5	10500	1111.0	1121.5	15500	2382.4	2397.1	20500	4077.9	4096.9	25500	6142.3	6164.6	30500	8515.7	8540.9	
600	2.6	3.1	5600	319.0	324.6	10600	1131.9	1142.5	15600	2412.0	2427.0	20600	4115.8	4134.7	25600	6186.9	6209.4	30600	8566.0	8591.2	
700	3.7	4.4	5700	330.5	336.4	10700	1153.0	1163.7	15700	2442.1	2457.3	20700	4153.8	4172.9	25700	6231.8	6254.3	30700	8616.2	8641.4	
800	5.0	5.8	5800	342.3	348.1	10800	1174.5	1185.2	15800	2472.6	2487.9	20800	4191.9	4210.8	25800	6276.8	6299.3	30800	8666.5	8691.7	
900	6.6	7.4	5900	354.2	360.1	10900	1195.8	1206.7	15900	2503.1	2518.4	20900	4229.9	4249.2	25900	6321.9	6344.4	30900	8716.8	8742.1	
	8.4	9.3																			
1000	10.3	11.3	6000	366.1	372.3	11000	1217.6	1228.5	16000	2533.6	2549.0	21000	4268.5	4287.9	26000	6367.0	6389.6	31000	8767.5	8793.0	
1100	12.4	13.5	6100	378.5	384.7	11100	1239.4	1250.4	16100	2564.4	2579.7	21100	4307.2	4326.6	26100	6412.3	6434.9	31100	8818.4	8843.9	
1200	14.7	16.0	6200	390.9	397.2	11200	1261.4	1272.6	16200	2595.2	2610.7	21200	4346.1	4365.4	26200	6457.7	6480.4	31200	8869.3	8894.8	
1300	17.3	18.7	6300	403.5	409.8	11300	1283.9	1295.2	16300	2626.4	2642.0	21300	4384.8	4404.4	26300	6503.1	6525.8	31300	8920.0	8945.4	
1400	20.1	21.5	6400	416.3	422.8	11400	1306.4	1317.7	16400	2657.6	2673.4	21400	4423.9	4443.4	26400	6548.8	6571.7	31400	8970.8	8996.4	
1500	23.0	24.6	6500	429.3	436.0	11500	1328.9	1340.2	16500	2689.1	2704.8	21500	4462.9	4482.6	26500	6594.6	6617.4				
1600	26.1	27.8	6600	442.6	449.3	11600	1351.6	1363.0	16600	2720.7	2736.6	21600	4502.4	4522.1	26600	6640.4	6663.4				
1700	29.5	31.3	6700	456.0	462.8	11700	1374.6	1386.2	16700	2752.5	2768.4	21700	4541.8	4561.7	26700	6686.3	6709.2				
1800	33.1	34.9	6800	469.7	476.6	11800	1397.9	1409.7	16800	2784.2	2800.2	21800	4581.6	4601.4	26800	6732.2	6755.2				
1900	36.8	38.8	6900	483.5	490.4	11900	1421.4	1433.2	16900	2816.3	2832.2	21900	4621.2	4641.1	26900	6778.3	6801.4				
2000	40.8	42.8	7000	497.4	504.6	12000	1444.9	1456.7	17000	2848.6	2864.8	22000	4661.2	4681.0	27000	6824.6	6847.9				
2100	45.0	47.2	7100	511.7	518.9	12100	1468.6	1480.6	17100	2881.2	2897.5	22100	4701.0	4721.0	27100	6871.3	6894.7				
2200	49.4	51.7	7200	526.0	533.3	12200	1492.7	1504.7	17200	2913.7	2930.2	22200	4741.2	4761.4	27200	6918.1	6941.5				
2300	54.0	56.4	7300	540.8	548.3	12300	1516.7	1528.7	17300	2946.5	2963.0	22300	4781.6	4801.9	27300	6964.8	6988.0				
2400	58.8	61.2	7400	555.8	563.2	12400	1540.9	1553.2	17400	2979.4	2995.8	22400	4822.1	4842.3	27400	7011.2	7034.5				
2500	63.7	66.4	7500	570.8	578.3	12500	1565.4	1577.7	17500	3012.3	3029.0	22500	4862.5	4882.8	27500	7057.9	7081.5				
2600	69.0	71.7	7600	585.9	593.5	12600	1590.0	1602.6	17600	3045.6	3062.3	22600	4903.3	4923.8	27600	7105.0	7128.7				
2700	74.4	77.2	7700	601.1	608.9	12700	1615.0	1627.5	17700	3079.0	3095.7	22700	4944.1	4964.5	27700	7152.3	7176.0				
2800	80.0	82.9	7800	616.9	624.8	12800	1640.0	1652.5	17800	3112.5	3129.4	22800	4985.0	5005.6	27800	7199.6	7223.3				
2900	85.8	88.8	7900	632.7	640.7	12900	1665.0	1677.6	17900	3146.4	3163.3	22900	5026.2	5046.9	27900	7247.0	7270.7				
3000	91.9	95.0	8000	648.7	656.7	13000	1690.4	1703.1	18000	3180.2	3197.3	23000	5067.7	5088.4	28000	7294.4	7318.0				
3100	98.1	101.2	8100	664.8	673.1	13100	1716.0	1729.0	18100	3214.5	3231.5	23100	5109.1	5129.8	28100	7341.8	7365.7				
3200	104.5	107.7	8200	681.4	689.5	13200	1741.9	1754.8	18200	3248.4	3265.4	23200	5150.5	5171.4	28200	7389.6	7413.5				
3300	111.0	114.5	8300	697.8	706.2	13300	1767.7	1780.8	18300	3282.5	3299.8	23300	5192.4	5213.3	28300	7437.5	7461.4				
3400	117.9	121.4	8400	714.5	723.0	13400	1794.0	1807.1	18400	3317.2	3334.4	23400	5234.1	5255.0	28400	7485.3	7509.3				
3500	125.0	128.5	8500	731.5	740.0	13500	1820.3	1833.4	18500	3351.9	3369.4	23500	5276.0	5297.0	28500	7533.4	7557.5				
3600	132.1	135.9	8600	748.5	757.2	13600	1846.6	1859.9	18600	3386.9	3404.4	23600	5318.1	5339.2	28600	7581.5	7605.6				
3700	139.6	143.4	8700	765.8	774.7	13700	1873.2	1886.5	18700	3421.8	3439.3	23700	5360.4	5381.5	28700	7629.7	7653.9				
3800	147.2	151.2	8800	783.6	792.4	13800	1899.8	1913.3	18800	3456.6	3474.1	23800	5402.7	5424.0	28800	7678.0	7702.2				
3900	155.2	159.2	8900	801.3	810.2	13900	1926.8	1940.5	18900	3491.7	3509.6	23900	5445.3	5466.6	28900	7726.4	7750.6				
4000	163.2	167.2	9000	819.1	828.2	14000	1954.1	1967.8	19000	3527.5	3545.4	24000	5487.9	5509.3	29000	7774.9	7799.3				
4100	171.4	175.6	9100	837.3	846.4	14100	1981.5	1995.2	19100	3563.3	3581.3	24100	5530.6	5552.1	29100	7823.7	7848.1				
4200	179.8	184.2	9200	855.6	864.8	14200	2008.8	2022.6	19200	3599.2	3617.2	24200	5573.6	5595.0	29200	7872.4	7896.9				
4300	188.5	192.9	9300	874.2	883.5	14300	2036.4	2050.4	19300	3635.1	3653.2	24300	5616.4	5638.0	29300	7921.4	7945.8				
4400	197.3	201.8	9400	892.9	902.3	14400	2064.3	2078.3	19400	3671.2	3689.2	24400	5659.6	5681.1	29400	7970.3	7994.7				
4500	206.4	211.0	9500	911.7	921.2	14500	2092.4	2106.6	19500	3707.2	3725.3	24500	5702.9	5724.7	29500	8019.2	8043.8				
4600	215.6	220.3	9600	930.7	940.2	14600	2120.8	2135.0	19600	3743.5	3761.6	24600	5746.4	5768.1	29600	8068.4	8093.1				
4700	225.0	229.9	9700	949.9	959.7	14700	2149.2	2163.4	19700	3779.9	3798.3	24700	5789.8	5811.5	29700	8117.8	8142.5				
4800	234.8	239.7	9800	969.5	979.2	14800	2177.7	2192.0	19800	3816.8	3835.3	24800	5833.3	5855.1	29800	8167.3	8192.1				
4900	244.6	249.6	9900	989.0	999.0	14900	2206.2	2220.6	19900	3853.8	3872.2	24900	5877.1	5899.0	29900	8216.9	8241.7				
5000	254.6	259.7	10000	1009.0	1019.0	15000	2235.1	2249.7	20000	3890.7	3909.2	25000	5920.8	5942.9	30000	8266.4	8291.2				



